Search For New And Unusual Strangeonia In Photoproduction Using CLAS†

Mukesh S. Saini

Advisor : Dr. Paul Eugenio
Department Of Physics, The Florida State University,
Tallahassee, FL

March 12, 2013

†Research funded by the US Department of Energy (DOE)

OUTLINE

- Meson Spectroscopy
- Experiment
- Data Selection
- Strangeonium Analysis
- Summary

Quantum chromodynamics (QCD) is theory of the strong interaction (color force).

It describes the interactions of the quarks and gluons making up the hadron

QCD Picture

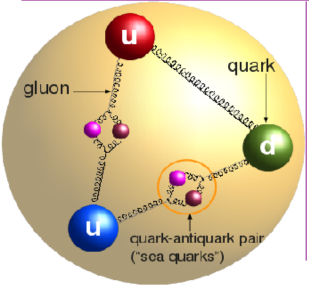

In constituent quark Model, →

Color charge!

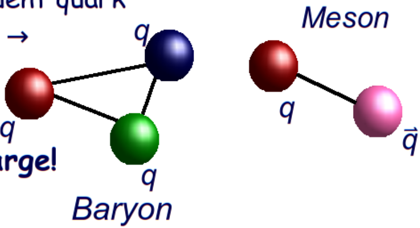

- Free quarks and gluons have not been observed in nature due to confinement.
- QCD predicts exotic hadrons beyond the naive quark model [hybrids, glueballs and multi-quark states]
- Mapping of the meson spectra will help us identify exotic unconventional mesons and decays, to further our insight into soft (Non-perturbative) QCD

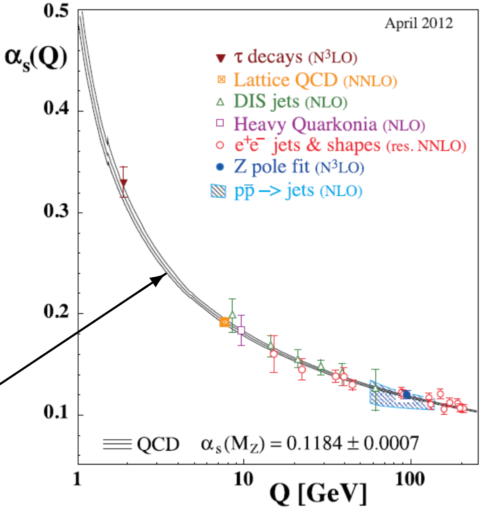

PDG, 2012

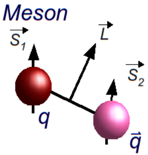

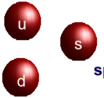

Light meson spectroscopy

$$\vec{J} = \vec{L} + \vec{S}$$

$$P = (-1)^{L+1}$$

$$C = (-1)^{L+S}$$

$$\mathrm{J}^{PC}\Big|_{allowed} = 0^{-+}, 0^{++}, 1^{--}, 1^{+-}, 1^{++}, 2^{--}, \ldots \ .$$

$$\mathrm{J}^{PC}\Big|_{exotic} = 0^{--}, 0^{+-}, 1^{-+}, 2^{+-}, 3^{-+}, \ldots \ .$$

Usual Mesons	EXOTICA			
Quark Model Mesons	Gluonic Hybrids	Tetra-quarks	Glue-Balls	...
$q\bar{q}$	$q\bar{q}g$	$q\bar{q}q\bar{q}$	gg	$\ldots$

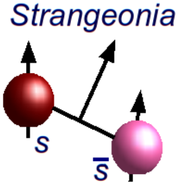

Image Source: WikiMedia Commons

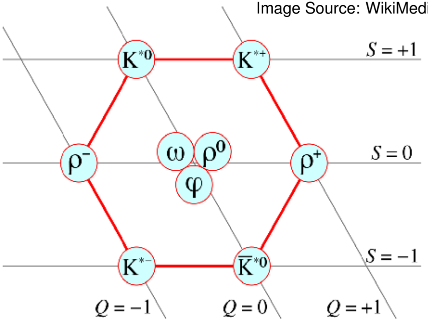

√ Of the 22 expected resonances from $^3P_0$ model predictions, only 7 candidates identified

$\eta - \eta'$	ϕ (1020)	h_1 (1380)†
f_1 (1420)	f_2' (1525)	ϕ (1680)
ϕ_3 (1850)	?	?

† Not Included in the PDG Summary Tables.

Expected Strangeonia spectrum

			J^{PC}	Name	Mass (MeV)
n=2	L=0	S=0	0^{-+}	η_s	1415
		S=1	1^{--}	ϕ	1680
	L=1	S=0	1^{+-}	h_1	1850
		S=1	0^{++}	f_0	2000
			1^{++}	f_1	1950
			2^{++}	f_2	2000
n=3	L=0	S=0	0^{-+}	η_s	1950
		S=1	1^{--}	ϕ	2050

← Radial excitations of (I = 0, $s\bar{s}$) meson.

			J^{PC}	Name	Mass (MeV)
n=1	L=0	S=0	0^{-+}	η,η'	548,958
		S=1	1^{--}	ϕ	1020
	L=1	S=0	1^{+-}	h_1'	1380
		S=1	0^{++}	f_0'	1500
			1^{++}	f_1'	1530
			2^{++}	f_2'	1525
	L=2	S=0	2^{-+}	η_2	1850
		S=1	1^{--}	ϕ_1	1850
			2^{--}	ϕ_2	1850
			3^{--}	ϕ_3	1854

← Orbital excitations of (I = 0, $s\bar{s}$) meson.

Tables from reference:
T. Barnes, N. Black and P. R. Page, Phys. Rev. D 68, 054014 (2003)

Why Study Strangeonia?

- Due to the intermediate mass of the strange quarks, study of the strangeonium states will serve as a bridge between short and large distance behavior of QCD confinement potential, a study of the transition from light quark sector to the HQET

How To Study Strangeonia

- “Due to the *OZI* rule, the observation of a state with a large branching fraction to $\eta\phi$, $\eta'\phi$ or $\phi\phi$ and small branches to nonstrange final states can serve as a “smoking gun" for an initial $s\bar{s}$ state." - Barnes, Black & Page (Strong decays of Strange Quarkonia)
- Open strangeness decay modes (KK, KK^*) for initial $s\bar{s}$ are susceptible to being confused with $n\bar{n}$, where $n \in \{u, d\}$, which can also decay via KK, KK^*
- $\phi\eta$ and $\phi\eta'$ decay modes are most likely to originate from an initial $s\bar{s}$ state, even though η has $n\bar{n}$ component

- In hadronic interactions, [$\gamma \iff \{\rho,\ \omega,\ \phi\}$] - with an important $s\bar{s}$ component - Vector Meson Dominance (VMD)
- Study of diffractive photoproduction reaction $\gamma\, p \rightarrow p\, \phi\, \eta$, should lead to observation of many C=-1 $s\bar{s}$ states
- If the decay products of a meson have a ϕ meson with another mostly strange meson like η, OZI rule dictates that initial state be $s\bar{s}$

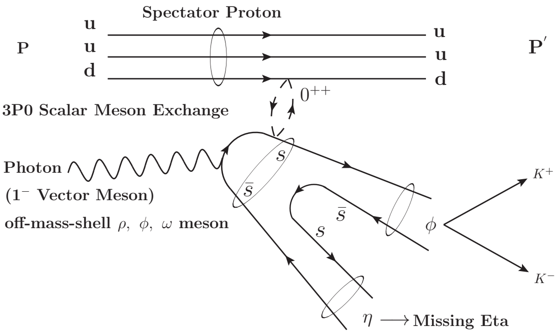

- In hadronic interactions, [$\gamma \iff \{\rho,\ \omega,\ \phi\}$] - with an important $s\bar{s}$ component - Vector Meson Dominance (VMD)
- Study of diffractive photoproduction reaction $\gamma\, p \rightarrow p\, \phi\, \eta$, should lead to observation of many C=-1 $s\bar{s}$ states
- If the decay products of a meson have a ϕ meson with another mostly strange meson like η, OZI rule dictates that initial state be $s\bar{s}$

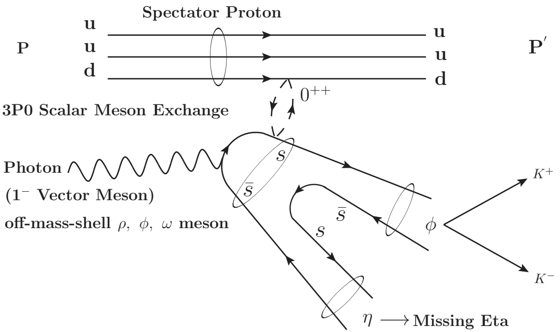

- In hadronic interactions, [$\gamma \iff \{\rho,\ \omega,\ \phi\}$] - with an important $s\bar{s}$ component - Vector Meson Dominance (VMD)
- Study of diffractive photoproduction reaction $\gamma\, p \rightarrow p\, \phi\, \eta$, should lead to observation of many C=-1 $s\bar{s}$ states
- If the decay products of a meson have a ϕ meson with another mostly strange meson like η, OZI rule dictates that initial state be $s\bar{s}$

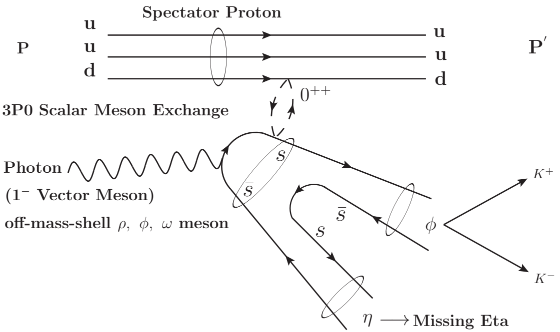

History - ϕ (1680) / X (1750)

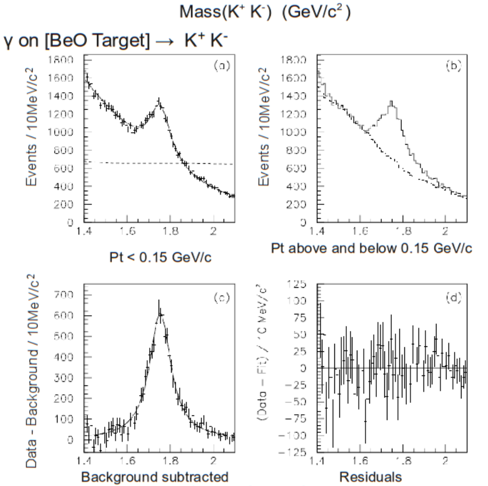

Image from reference:
J. M. Link et al., [FOCUS Collaboration], Phys. Lett. B 545, 50 (2002)

FOCUS Experiment

- e^+e^- annhilation observe $\phi(1680)$ in KK^* decay
- Photoproduction experiments observe a resonance at 1750 MeV/c^2 in $X(1750) \to K^+K^-$
- Earlier photoproduction results had low statistics $\sim$ few 100 events
- FOCUS@Fermilab has 11,700 $X(1750) \to K^+K^-$
- FOCUS studied $KK : KK^*$ branching ratio and claimed $X(1750) \neq \phi(1680)$
- If $X(1750) \in \{s\bar{s}\}$, cleanest way to observe it will be $X \to \phi\eta$

Strangeonia Status

Strangeonium State		Predicted Decay Width Theory MeV/c^2
$\phi(1680)$	2S	$\Gamma_{theory} = 378$ $\Gamma_{\phi\eta} = 44$
$\phi(2050)$	3S	$\Gamma_{theory} = 378$ $\Gamma_{\phi\eta} = 21$
$h_1(1850)$	2P	$\Gamma_{theory} = 193$ $\Gamma_{\phi\eta} = 33$
$\phi_3(1854)$	1D	$\Gamma_{theory} = 104$ $\Gamma_{\phi\eta} = 3$
$\phi_2(1850)$	1D	$\Gamma_{theory} = 214$ $\Gamma_{\phi\eta} = 53$
$\phi(1850)$	1D	$\Gamma_{theory} = 652$ $\Gamma_{\phi\eta} = 29$
$h_3(2200)$	1F	$\Gamma_{theory} = 249$ $\Gamma_{\phi\eta} = 5$

Experimentally Observed States

- Only 2 of these claimed $s\bar{s}$ observed
  - In e^+e^- exp. - $\phi(1680) \rightarrow KK^*$ $\Gamma_{measured} = 150 \pm 50$ MeV/c^2
  - In pK^- exp. - $\phi_3(1850) \rightarrow K^+K^-$ $\Gamma_{measured} = 87^{+28}_{-23}$ MeV/c^2
- All existing $s\bar{s}$ observations in open strangeness decay modes
- Lack of observed $s\bar{s}$ states implies lots of potential for physics discovery

- Theoretical predictions for $s\bar{s}$ expected to be observed in the $\phi\ \eta$ invariant mass distribution from the reference - T. Barnes, N. Black and P. R. Page, Phys. Rev. D 68, 054014 (2003)

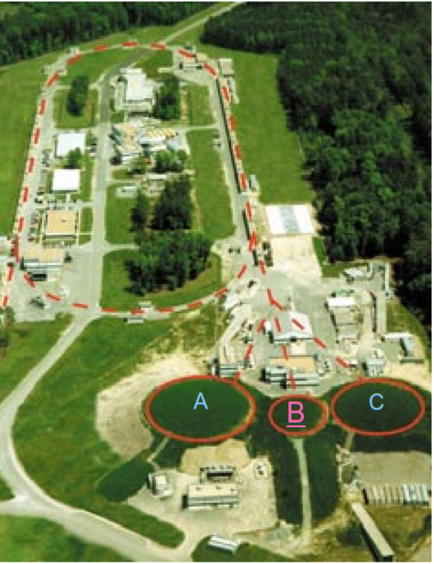

- **CEBAF**:
  Continuous **E**lectron **B**eam **A**ccelerator **F**acility,
  hosted at
  Thomas Jefferson National Accelerator Facility,
  Newport News, Virginia
- CEBAF delivers e^- beams to the 3 Halls, polarised upon request in 5 passes with e^- Energies up-to 6 GeV (1.2 x 5)
- Hall-B is the smallest experimental Hall with the largest detector "CLAS"
- Major upgrades at CEBAF and the Halls for the 12 GeV upgrade as well as addition of a new Hall-D which will house GLUEX created with meson spectroscopy as the primary purpose

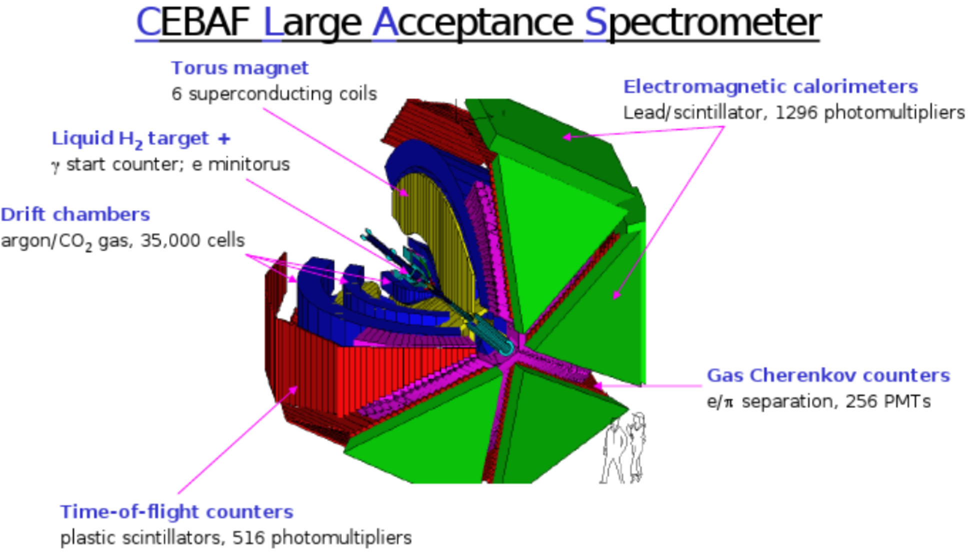
CEBAF Large Acceptance Spectrometer
Torus magnet
6 superconducting coils
Electromagnetic calorimeters
Lead/scintillator, 1296 photomultipliers
Liquid H2 target +
γ start counter; e minitorus
Drift chambers
argon/CO2 gas, 35,000 cells
Gas Cherenkov counters
e/π separation, 256 PMTs
Time-of-flight counters
plastic scintillators, 516 photomultipliers

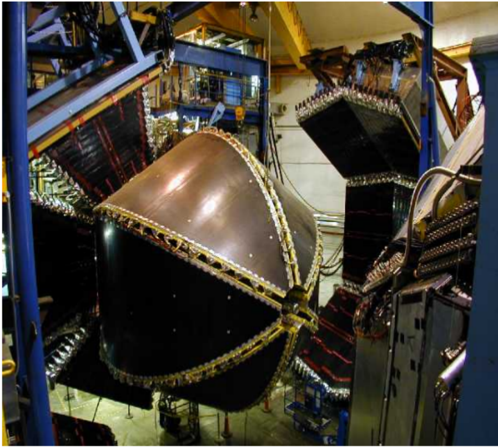

- Skeletal superconducting Toroidal Magnets for CLAS.
- CLAS detector during assembly.

- 44.2 Days of beam-time over 70 days, 1^{st} April to 9^{th} June, 2008
- Beam current $\rightarrowtail$ 60-65 nA ; $E_e \rightarrowtail 5.71 GeV$; DAQ Rate $\rightarrowtail$ 8 KHz
- 26.2 billion triggers; Main Trigger $\rightarrowtail$ 2 prong or more with $E_\gamma \geq 4.4$ GeV, 3 prong with no MOR ...
- 126 TB of raw data
- 250 TB of reconstructed data
- 68 pb^{-1} of photoproduction data

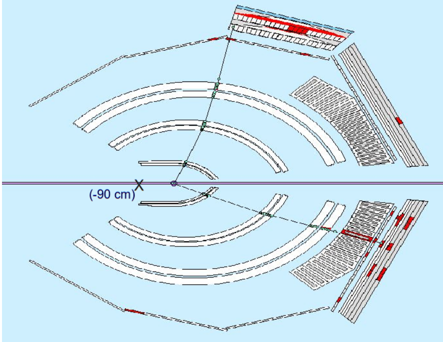

Detector Calibrations

- Start Counter - Mukesh Saini
- Tagger - Mukesh Saini
- Time Of Flight - Craig Bookwalter
- Drift Chamber - Diane Schott
- Reconstruction - Johann Goetz

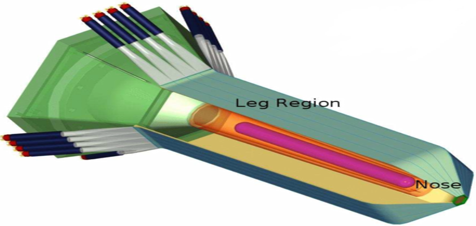

- Incorporates the independent sector based tracking of CLAS
- g12 pulled ST 90cm back from the center of CLAS to increase acceptance for low t, forward going particles
- ST crucial for picking the right photon and Particle ID

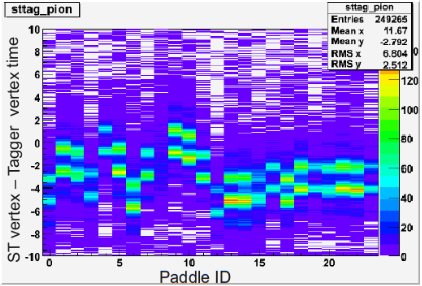

(a) Before

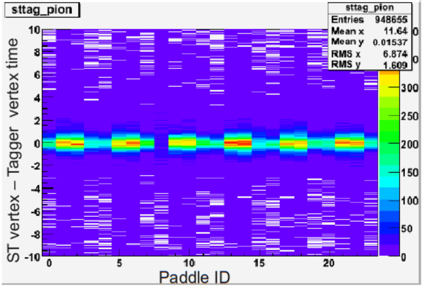

(b) After

Start Counter calibrated by Mukesh Saini

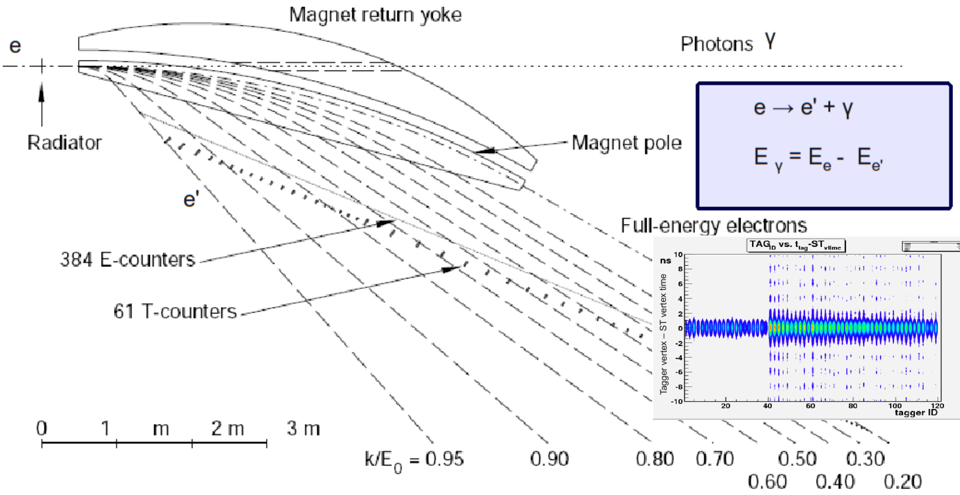

$$e \rightarrow e' + \gamma$$

$$E_\gamma = E_e - E_{e'}$$

Fig. 23. Hall B photon-tagging system.

Tagging system calibrated by Mukesh Saini

Particle Selection

- 3 charged particle tracks detected in CLAS - $\mathrm{Proton},\ \mathrm{K}^+,\ \mathrm{K}^-$
- Apply energy-momentum conservation - $\gamma_\mu + P_\mu = P'_\mu + K^+_\mu + K^-_\mu + MM_\mu$
- Select - η - in the missing mass distribution
- Add four-vectors for K^+K^- to get their invariant mass and hence identify the - ϕ - meson
- Reconstruct the invariant mass for ($\phi\eta$) using the above selected ϕ & η mesons

Meson ID

- To Identify ϕ, Select 1010 MeV $\leq$ IM(K^+ K^-) $\leq$ 1030 MeV
- To identify η, Select 510 MeV $\leq$ MM $\leq$ 580 MeV

Cuts

- Event vertex time within 1.002 ns of the Start Counter vertex time
- All particles have the difference between their measured and calculated 'β' less than 0.05
- Event vertex is required to be within the Target

Vertex Distribution for Z and X-Y plane

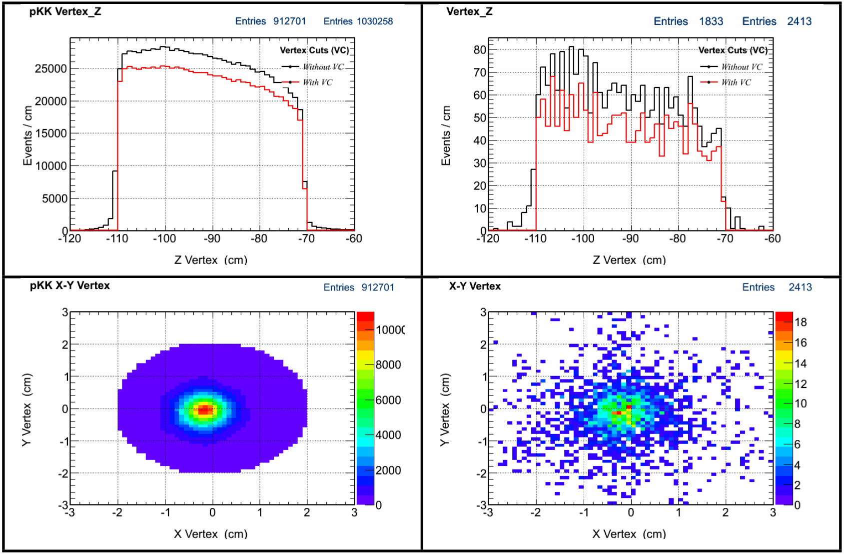

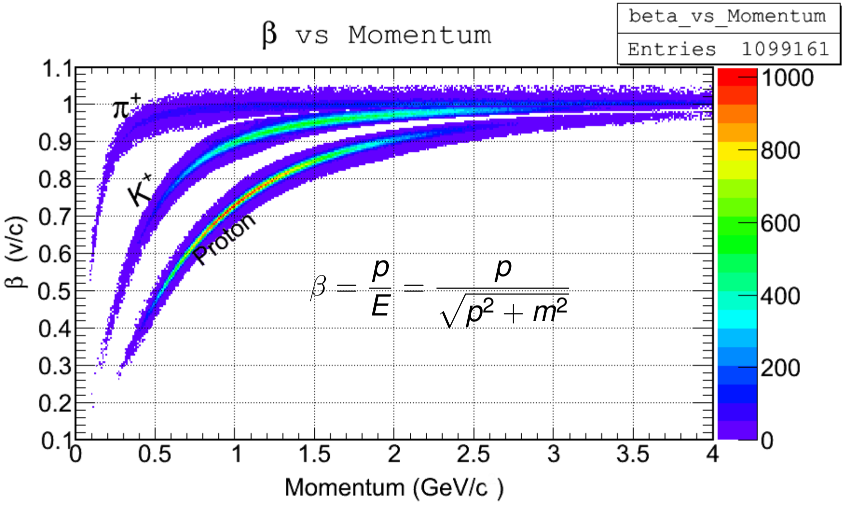
β vs Momentum
beta_vs_Momentum
Entries 1099161
π+
K+
Proton
$\beta = \frac{p}{E} = \frac{p}{\sqrt{p^2 + m^2}}$
β (v/c)
Momentum (GeV/c)
1.1
1
0.9
0.8
0.7
0.6
0.5
0.4
0.3
0.2
0.1
0
0.5
1
1.5
2
2.5
3
3.5
4
1000
800
600
400
200
0

β Vs Momentum Distributions

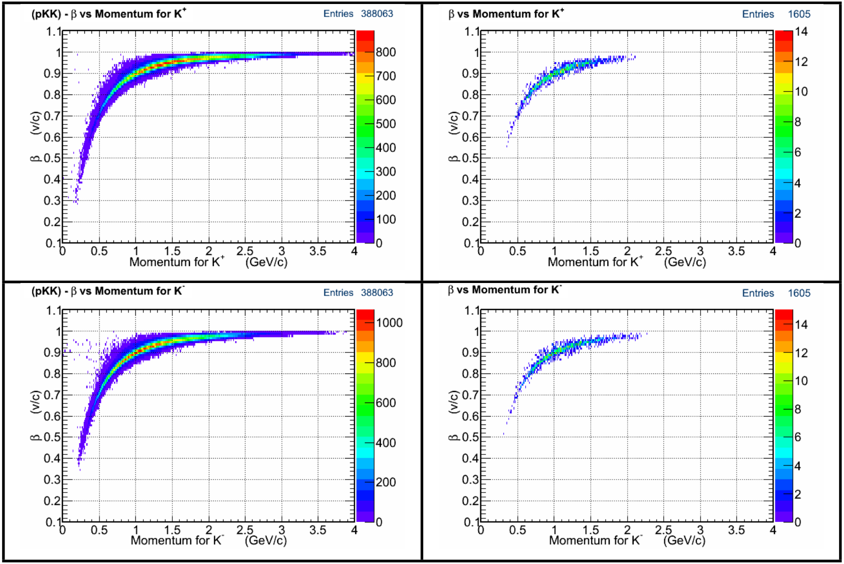

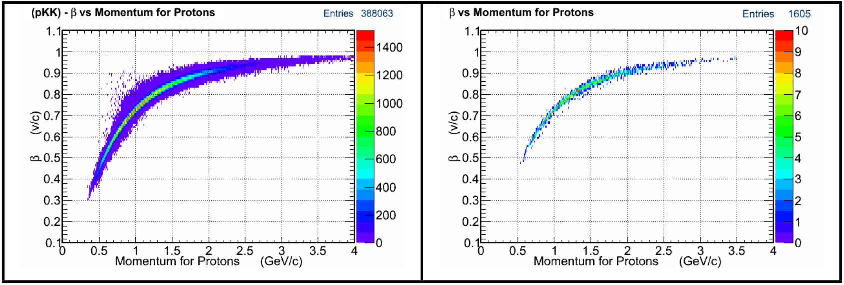

Observations

- Vertex and Timing Distributions are acceptable
- β for *Proton*, K^+ & K^- have no cross-contamination bands
- PID and Cuts employed work reasonably well

$$\gamma \; + \; \textit{proton} \; \rightarrowtail \; \textit{proton} \; + \; \phi \; + \; \eta$$

$$\gamma \; + \; \textit{proton} \; \rightarrowtail \; \textit{proton} \; + \; K^{+} \; + \; K^{-} \; + \; [\eta]$$

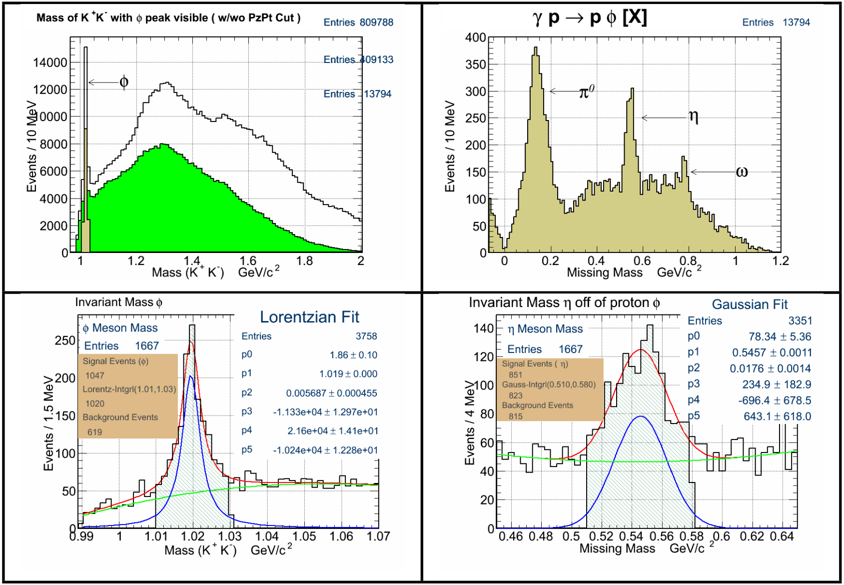
Mass of K⁺K⁻ with ϕ peak visible (w/wo PzPt Cut)
Entries 809788
Entries 409133
Entries 13794
ϕ
Events / 10 MeV
Mass (K⁺ K⁻) GeV/c²
γ p → p ϕ [X]
Entries 13794
π⁰
η
ω
Events / 10 MeV
Missing Mass GeV/c²
Invariant Mass ϕ
ϕ Meson Mass
Entries 1667
Signal Events (ϕ) 1047
Lorentz-Intgrl(1.01,1.03) 1020
Background Events 619
Lorentzian Fit
Entries 3758
p0 1.86 ± 0.10
p1 1.019 ± 0.000
p2 0.005687 ± 0.000455
p3 -1.133e+04 ± 1.297e+01
p4 2.16e+04 ± 1.41e+01
p5 -1.024e+04 ± 1.228e+01
Events / 1.5 MeV
Mass (K⁺ K⁻) GeV/c²
Invariant Mass η off of proton ϕ
η Meson Mass
Entries 1667
Signal Events (η) 851
Gauss-Intgrl(0.510,0.580) 823
Background Events 815
Gaussian Fit
Entries 3351
p0 78.34 ± 5.36
p1 0.5457 ± 0.0011
p2 0.0176 ± 0.0014
p3 234.9 ± 182.9
p4 -696.4 ± 678.5
p5 643.1 ± 618.0
Events / 4 MeV
Missing Mass GeV/c²

$$\text{Mandelstam's } t = |P^{\mu}_{\gamma} - P^{\mu}_{X}|^2 = |P^{\mu}_{\text{target}} - P^{\mu}_{\text{recoil}}|^2$$

$$t' = t - t_{min}, \text{ where } t_{min} = \text{Minimum Four-Momentum Transfer Squared Required For Resonance Production}$$

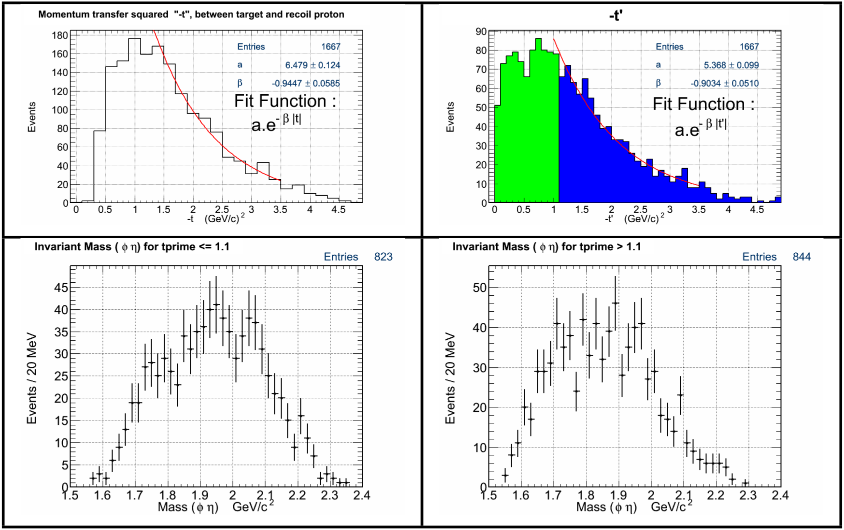

Selection Based On Kinematics

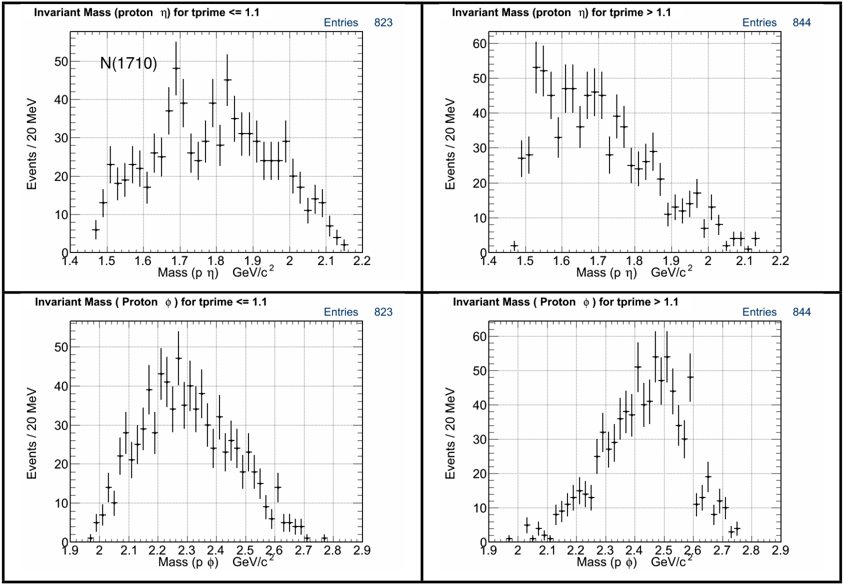

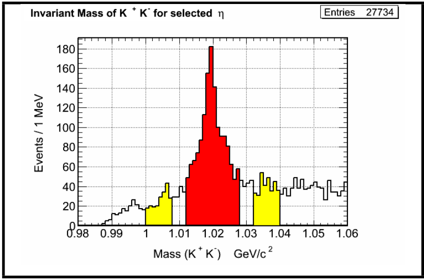

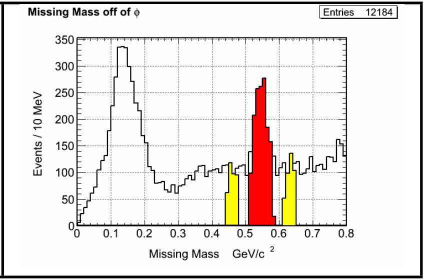

Side-Band Observations:

- ϕ width is 4 MeV and the peak is at 1020 MeV
- η width is 17 MeV and the peak is at 547 MeV
- Signal region is chosen to be peak $\pm 2\sigma$
- $\phi \rightarrow 1012 - 1028$ MeV, $\eta \rightarrow 513 - 581$ MeV
- Gap of 1σ is used between signal and sideband to minimize loss of ϕ's
- Gap of 2σ is used between signal and sideband to minimize loss of η's

Elliptical Sideband Selection

$$\left(\frac{x - \phi_{mass}}{\frac{\phi \text{ mass range}}{2}}\right)^2 + \left(\frac{y - \eta_{mass}}{\frac{\eta \text{ mass range}}{2}}\right)^2 = 1$$

ϕ mass	1.0195 GeV/c^2
ϕ mass range selected	0.0019 GeV/c^2
ϕ sideband mass gap selected	$\sqrt{3}\times$ 0.0019 GeV/c^2
ϕ sideband mass range selected	$2\times$ 0.0019 GeV/c^2
η mass	0.5478 GeV/c^2
η mass range selected	0.070 GeV/c^2
η sideband mass gap selected	$\sqrt{3}\times$ 0.070 GeV/c^2
η sideband mass range selected	$2\times$ 0.070 GeV/c^2

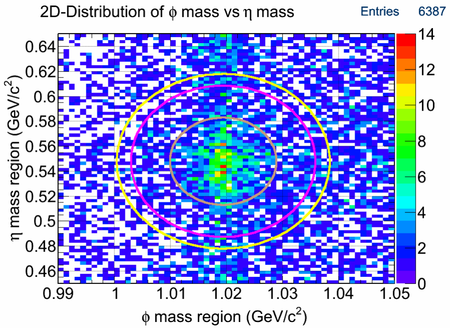

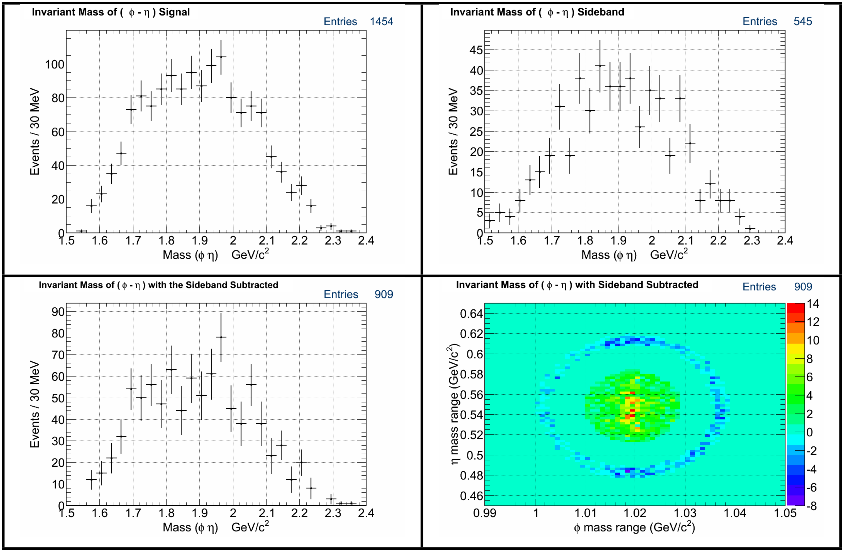
Invariant Mass of (ϕ - η) Signal
Entries 1454
Events / 30 MeV
Mass (ϕ η) GeV/c2
Invariant Mass of (ϕ - η) Sideband
Entries 545
Events / 30 MeV
Mass (ϕ η) GeV/c2
Invariant Mass of (ϕ - η) with the Sideband Subtracted
Entries 909
Events / 30 MeV
Mass (ϕ η) GeV/c2
Invariant Mass of (ϕ - η) with Sideband Subtracted
Entries 909
η mass range (GeV/c2)
ϕ mass range (GeV/c2)

Cross Section Formulae

$$\frac{N_{target}}{V} = 2 \times N_{avogadro} \times \frac{\rho_{target}}{A_{H_2}}$$

$$\frac{N_{observed}}{Acceptance} = \sigma \times N_{incident} \times N_{target}$$

$$\sigma = \frac{N_{observed} \times A_{H_2}}{2 \times N_{incident} \times N_{avogadro} \times \rho_{target} \times L_{target} \times Acceptance}$$

where,

N_{target}	is	the number of target protons that on average lie in the path of the incoming beam photons,
$N_{observed}$	is	the number of observed events in the experiment, aka the yield,
ρ_{target}	is	the density of the LH_2 used in the experiment,
$N_{incident}$	is	the integrated flux (total number) of the incoming beam photons that were incident on the target to achieve the observed yield,
L_{target}	is	the length of the target cell,
Acceptance	is	derived from the simulations of the reaction phase space for the experiment and represents the corrections due to the finite acceptance of the detector.

Cross Section

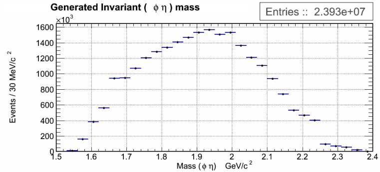

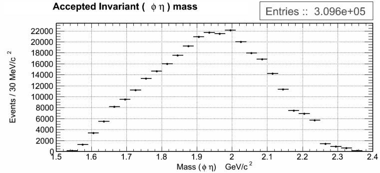

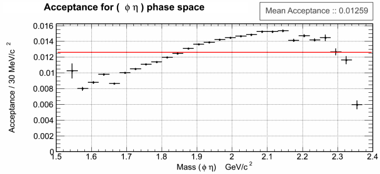

Measured Yield of $\phi\ \eta$ events	909 ± 45
Reconstruction inefficiency at 60 nA	16%
ST inefficiency per charged track	6%
Branching ratio $\phi \rightarrow K^+K^-$	$48.5\% \pm 0.5\%$
Corrected Yield of $\phi\ \eta$ events	2686 ± 133
E_γ Flux (10^{13})	2.18 ± 0.17
Overall phase space $\phi\ \eta$ MC Acceptance	1.26%
Systematic error - $\phi\ \eta$ simulations	7.9%
Systematic error - Sideband Subtraction	0.8%
Systematic error - PID	1.3%
Systematic error - Photon Flux Normalisation	7.9 %
Systematic error - Miscellaneous	0.26%
Conservative total systematic error	12.5%

Cross section - $\sigma_{X \rightarrow \phi\eta}$ for $E_\gamma \in \{4.40, 5.45\}$

- 5.8 ± 0.3 (stat) ± 0.72 (sys) nb

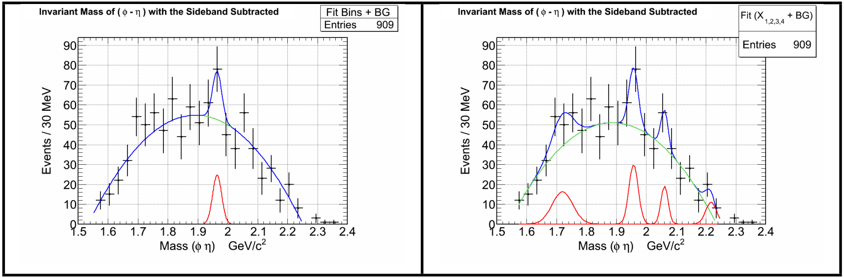

Feldman-Cousins Method

- Establishing discovery requires rejecting the background only hypothesis
- Particle physics experiments - 3σ signal significance $\rightarrowtail$ evidence, 5σ signal significance $\rightarrowtail$ discovery
- FeldmanCousins method - a frequentist approach, uses relative frequency of an event - Perform multiple experiments and number of positive results determines probability of that result
- It uses only the observed number of events and the estimated background count to calculate the confidence limits
- The fixed-unknown-true value will fall within the confidence interval in 90% of the repeats of the same experiment

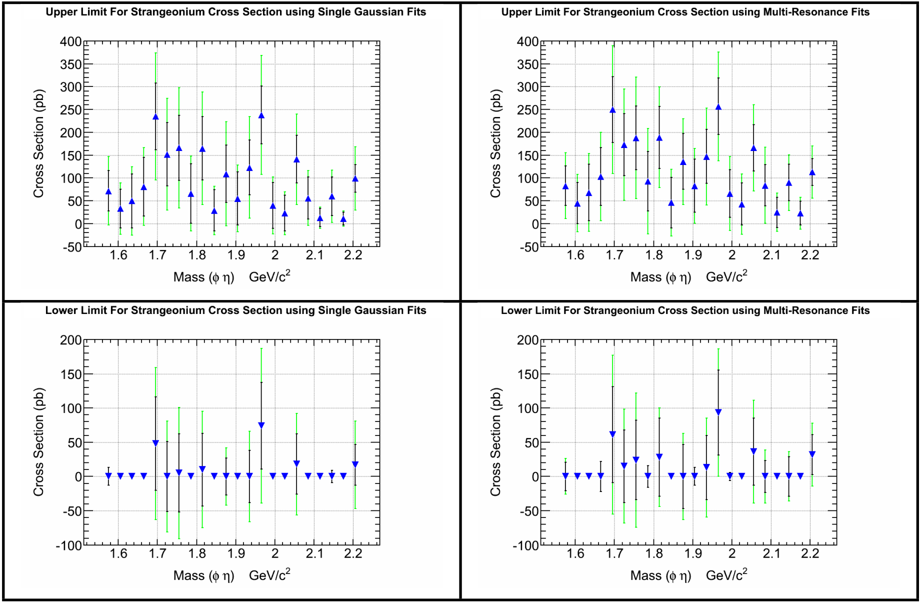
Upper Limit For Strangeonium Cross Section using Single Gaussian Fits
Upper Limit For Strangeonium Cross Section using Multi-Resonance Fits
Lower Limit For Strangeonium Cross Section using Single Gaussian Fits
Lower Limit For Strangeonium Cross Section using Multi-Resonance Fits
Cross Section (pb)
Mass (ϕ η) GeV/c2

- The two known and expected resonances - $\phi(1680)$ and $\phi_3(1850)$ - were not observed in the $\phi\ \eta$ invariant mass spectrum
- Largest cross section upper limit for strangeonium decay - '$s\bar{s} \rightarrow \phi\ \eta$'
  - 1695 MeV/c^2 - 250 pb
  - 1965 MeV/c^2 - 250 pb
- Calculated lower limits for $s\bar{s} \rightarrow \phi\ \eta$ consistent with zero

Comment on X(1750)

- Omega spectrometer measured X(1750) $\rightarrow K^+K^-$ photoproduction cross section at E$_\gamma$ = 45 GeV/c^2 to be 8 $\pm$ 3 nb
- $^3P_0$ model predicts the branching ratio of $K^+K^- : \phi\ \eta$ to be 2 : 1
- Extrapolating using froissart bound, the state is expected at least at a level of 1 nb
- If photoproduced X(1750) $\rightarrow K^+K^- \in \{s\bar{s}\}$, Our analysis would have observed the state in $\phi\ \eta$ at a level well above 250 pb
- The analysis thus supports FOCUS's claim that X(1750) $\neq \phi(1680)$

Observations From $\phi\ \eta$ Cross Section Study

- The two known and expected resonances - $\phi(1680)$ and $\phi_3(1850)$ - were not observed in the $\phi\ \eta$ invariant mass spectrum
- Largest cross section upper limit for strangeonium decay - '$s\bar{s} \rightarrow \phi\ \eta$'
  - 1695 MeV/c^2 - 250 pb
  - 1965 MeV/c^2 - 250 pb
- Calculated lower limits for $s\bar{s} \rightarrow \phi\ \eta$ consistent with zero

Comment on X(1750)

- Omega spectrometer measured X(1750) $\rightarrow K^+K^-$ photoproduction cross section at E$_\gamma$ = 45 GeV/c^2 to be 8 $\pm$ 3 nb
- $^3P_0$ model predicts the branching ratio of $K^+K^- : \phi\ \eta$ to be 2 : 1
- Extrapolating using froissart bound, the state is expected at least at a level of 1 nb
- If photoproduced X(1750) $\rightarrow K^+K^- \in \{s\bar{s}\}$, Our analysis would have observed the state in $\phi\ \eta$ at a level well above 250 pb
- The analysis thus supports FOCUS's claim that X(1750) $\neq \phi(1680)$

- The two known and expected resonances - ϕ(1680) and ϕ_3(1850) - were not observed in the $\phi\ \eta$ invariant mass spectrum
- Largest cross section upper limit for strangeonium decay - '$s\bar{s} \rightarrow \phi\ \eta$'
  - 1695 MeV/c^2 - 250 pb
  - 1965 MeV/c^2 - 250 pb
- Calculated lower limits for $s\bar{s} \rightarrow \phi\ \eta$ consistent with zero

Comment on X(1750)

- Omega spectrometer measured X(1750) $\rightarrow K^+K^-$ photoproduction cross section at E$_\gamma$ = 45 GeV/c^2 to be 8 $\pm$ 3 nb
- $^3P_0$ model predicts the branching ratio of K^+K^- : $\phi\ \eta$ to be 2 : 1
- Extrapolating using froissart bound, the state is expected at least at a level of 1 nb
- If photoproduced X(1750) $\rightarrow K^+K^- \in \{s\bar{s}\}$, Our analysis would have observed the state in $\phi\ \eta$ at a level well above 250 pb
- The analysis thus supports FOCUS's claim that X(1750) $\neq \phi$(1680)

- The two known and expected resonances - $\phi(1680)$ and $\phi_3(1850)$ - were not observed in the $\phi\ \eta$ invariant mass spectrum
- Largest cross section upper limit for strangeonium decay - '$s\bar{s} \to \phi\ \eta$'
  - 1695 MeV/c^2 - 250 pb
  - 1965 MeV/c^2 - 250 pb
- Calculated lower limits for $s\bar{s} \to \phi\ \eta$ consistent with zero

Comment on X(1750)

- Omega spectrometer measured X(1750) $\to K^+K^-$ photoproduction cross section at E$_\gamma$ = 45 GeV/c^2 to be 8 $\pm$ 3 nb
- $^3P_0$ model predicts the branching ratio of $K^+K^- : \phi\ \eta$ to be 2 : 1
- Extrapolating using froissart bound, the state is expected at least at a level of 1 nb
- If photoproduced X(1750) $\to K^+K^- \in \{s\bar{s}\}$, Our analysis would have observed the state in $\phi\ \eta$ at a level well above 250 pb
- The analysis thus supports FOCUS's claim that X(1750) $\neq \phi(1680)$

- The two known and expected resonances - $\phi(1680)$ and $\phi_3(1850)$ - were not observed in the $\phi\,\eta$ invariant mass spectrum
- Largest cross section upper limit for strangeonium decay - '$s\bar{s} \to \phi\,\eta$'
  - 1695 MeV/c^2 - 250 pb
  - 1965 MeV/c^2 - 250 pb
- Calculated lower limits for $s\bar{s} \to \phi\,\eta$ consistent with zero

Comment on X(1750)

- Omega spectrometer measured X(1750) $\to K^+K^-$ photoproduction cross section at E_γ = 45 GeV/c^2 to be 8 $\pm$ 3 nb
- $^3P_0$ model predicts the branching ratio of $K^+K^- : \phi\,\eta$ to be 2 : 1
- Extrapolating using froissart bound, the state is expected at least at a level of 1 nb
- If photoproduced X(1750) $\to K^+K^- \in \{s\bar{s}\}$, Our analysis would have observed the state in $\phi\,\eta$ at a level well above 250 pb
- The analysis thus supports FOCUS's claim that X(1750) $\neq \phi(1680)$

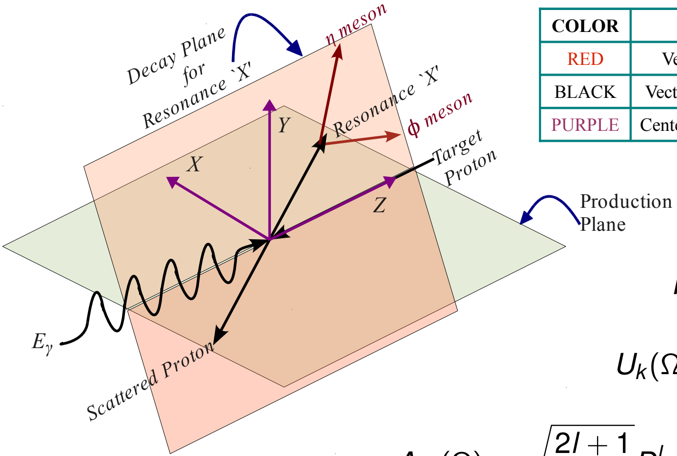

COLOR	ATTRIBUTE
RED	Vectors In Decay Plane
BLACK	Vectors In Production Plane
PURPLE	Center of Mass Frame's Axes

$$I(\Omega) = \sum_k \left| U_k(\Omega) \right|^2$$

$$U_k(\Omega) = \sum_{lm} V_{lmk} A_{lm}(\Omega)$$

$$A_{lm}(\Omega) = \sqrt{\frac{2l+1}{4\pi}} D^{l}_{m0}{}^{*}(\phi, \theta, 0) = Y^m_l(\Omega)$$

$$I(\tau) \propto \sum_k \left| \sum_\alpha V_{k\alpha} A_\alpha(\tau) \right|^2$$

$$\alpha \ \forall \ \{J, P, C, M, L, l, (w, \Gamma)\}$$

Fourier Expansion :

$$f(x) = \frac{a_0}{2} + \sum_{n=1}^{\infty} (a_n sin(nx) + b_n cos(nx))$$

+ve Reflectivity $JPCM + L$	-ve Reflectivity $JPCM - L$
$1 + -1 + D$	$1 + -1 - D$
$1 - -1 + P$	$1 - -1 - P$
$1 + -1 + S$	$1 + -1 - S$
$2 - -1 + F$	$2 - -1 - F$
$2 - -1 + P$	$2 - -1 - P$
$3 - -1 + F$	$3 - -1 - F$

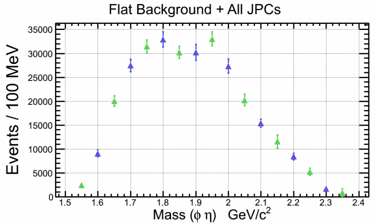

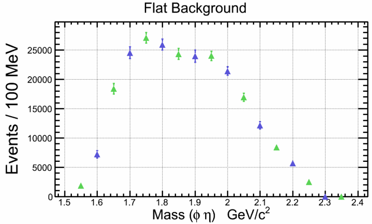

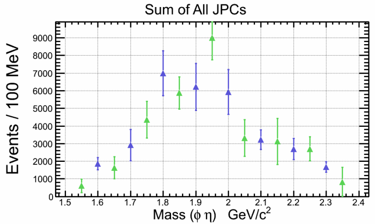

- Displayed fits are for $\phi\ \eta$ data binned in 100 MeV bins - then rebinned again in 100 MeV bins with an offset of 50 MeV - color coded by green and blue
- Data four-vectors used for PWA were kinematically fitted to a missing η
- Extended maximum likelihood method was implemented using minuit to maximize the likelihood of describing the decay angular distributions using the waveset shown

Minimal PWA Waveset

+ve Reflectivity $JPCM + L$	-ve Reflectivity $JPCM - L$
$1 + -1 + D$	$1 + -1 - D$
$1 - -1 + P$	$1 - -1 - P$
$1 + -1 + S$	$1 + -1 - S$
$2 - -1 + F$	$2 - -1 - F$
$2 - -1 + P$	$2 - -1 - P$
$3 - -1 + F$	$3 - -1 - F$

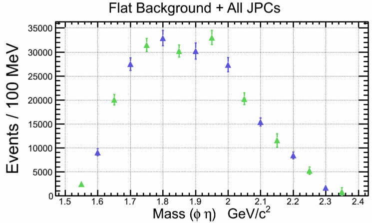

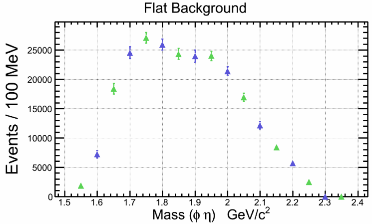

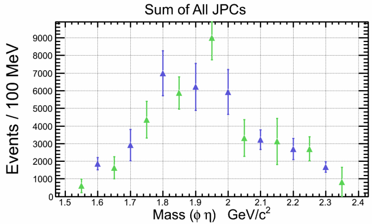

- Displayed fits are for $\phi\ \eta$ data binned in 100 MeV bins - then rebinned again in 100 MeV bins with an offset of 50 MeV - color coded by green and blue
- Data four-vectors used for PWA were kinematically fitted to a missing η
- Extended maximum likelihood method was implemented using minuit to maximize the likelihood of describing the decay angular distributions using the waveset shown

+ve Reflectivity $JPCM + L$	-ve Reflectivity $JPCM - L$
$1 + -1 + D$	$1 + -1 - D$
$1 - -1 + P$	$1 - -1 - P$
$1 + -1 + S$	$1 + -1 - S$
$2 - -1 + F$	$2 - -1 - F$
$2 - -1 + P$	$2 - -1 - P$
$3 - -1 + F$	$3 - -1 - F$

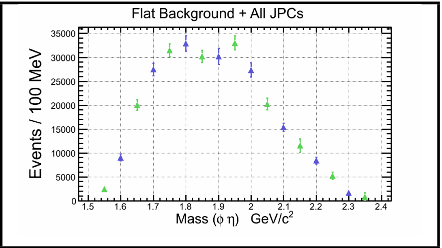

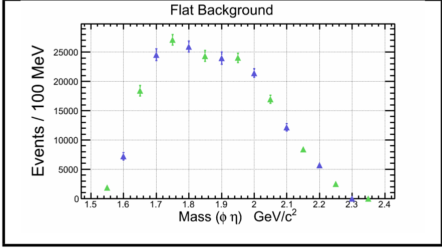

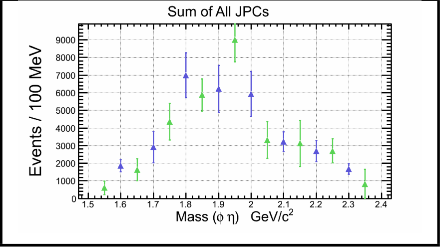

- Displayed fits are for $\phi\ \eta$ data binned in 100 MeV bins - then rebinned again in 100 MeV bins with an offset of 50 MeV - color coded by green and blue
- Data four-vectors used for PWA were kinematically fitted to a missing η
- Extended maximum likelihood method was implemented using minuit to maximize the likelihood of describing the decay angular distributions using the waveset shown

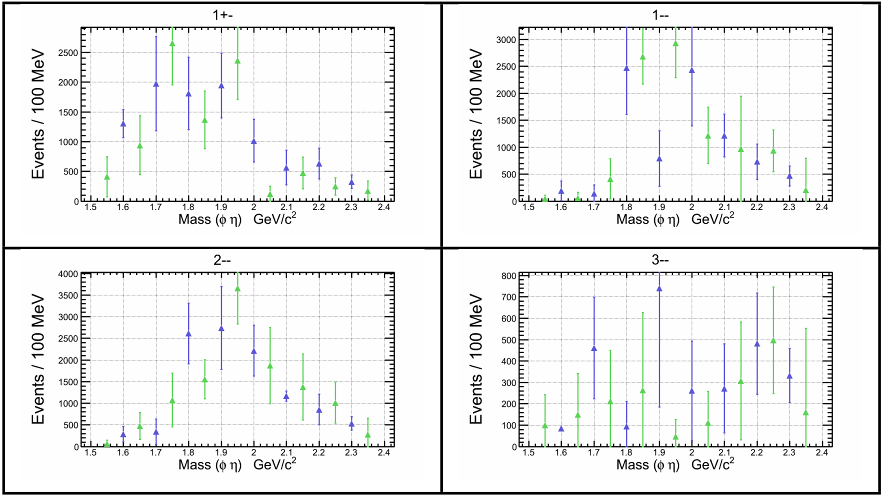

- 2 − − wave is stable; but not much stronger than any other JPC
- No JPC is singularly preferred in the PWA analysis; PWA inconclusive about the makeup of the observed spectra

- We acquired the world's largest photoproduction dataset for $\phi\,\eta$
  - 909 ± 45 $\phi\,\eta$ events
- First cross section measurement for '$\gamma\,p \;\rightarrow\; p\,X \;\rightarrow\; p\,\phi\,\eta$'
  - 5.8 ± 0.3 (stat) $\pm\, 0.72$ (sys) nb for $E_\gamma \in \{4.40, 5.45\}$
- No statistically significant resonant structure observed in $\phi\,\eta$ invariant mass distribution
- First calculations of upper limits on '$\gamma\,p \;\rightarrow\; p\,X \;\rightarrow\; p\,\phi\,\eta$'
  - Upper limit for $\phi(1680)$ - 140 pb
  - Upper limit for $\phi_3(1850)$ - 60 pb
  - Upper limit for X(1750) supports X(1750) $\notin \{s\bar{s}\} \neq \phi(1680)$
  - Largest cross section upper limit is observed to be 250 pb
- Strangeonia photoproduction cross sections - measured in their golden decay mode $\phi\,\eta$ - are much lower than expected
  - Assumptions of this analysis are suspect
  - Strangeonia are rarer than expected; more statistics needed
  - Search for strangeonia continues. . .

- We acquired the world's largest photoproduction dataset for $\phi\,\eta$
  - 909 ± 45 $\phi\,\eta$ events
- First cross section measurement for '$\gamma\, p \;\rightarrow\; p\, X \;\rightarrow\; p\, \phi\, \eta$'
  - 5.8 ± 0.3 (stat) $\pm\ 0.72$ (sys) nb for $E_\gamma \in \{4.40, 5.45\}$
- No statistically significant resonant structure observed in $\phi\,\eta$ invariant mass distribution
- First calculations of upper limits on '$\gamma\, p \;\rightarrow\; p\, X \;\rightarrow\; p\, \phi\, \eta$'
  - Upper limit for $\phi(1680)$ - 140 pb
  - Upper limit for $\phi_3(1850)$ - 60 pb
  - Upper limit for X(1750) supports X(1750) $\notin \{s\bar{s}\} \neq \phi(1680)$
  - Largest cross section upper limit is observed to be 250 pb
- Strangeonia photoproduction cross sections - measured in their golden decay mode $\phi\,\eta$ - are much lower than expected
  - Assumptions of this analysis are suspect
  - Strangeonia are rarer than expected; more statistics needed
  - Search for strangeonia continues...

Summary

- We acquired the world's largest photoproduction dataset for $\phi\,\eta$
  - 909 ± 45 $\phi\,\eta$ events
- First cross section measurement for '$\gamma\, p \rightarrow\, p\, X \rightarrow\, p\, \phi\, \eta$'
  - 5.8 ± 0.3 (stat) $\pm$ 0.72 (sys) nb for $E_\gamma \in \{4.40, 5.45\}$
- No statistically significant resonant structure observed in $\phi\,\eta$ invariant mass distribution
- First calculations of upper limits on '$\gamma\, p \rightarrow\, p\, X \rightarrow\, p\, \phi\, \eta$'
  - Upper limit for $\phi(1680)$ - 140 pb
  - Upper limit for $\phi_3(1850)$ - 60 pb
  - Upper limit for X(1750) supports X(1750) $\notin \{s\bar{s}\} \neq \phi(1680)$
  - Largest cross section upper limit is observed to be 250 pb
- Strangeonia photoproduction cross sections - measured in their golden decay mode $\phi\,\eta$ - are much lower than expected
  - Assumptions of this analysis are suspect
  - Strangeonia are rarer than expected; more statistics needed
  - Search for strangeonia continues. . .

Summary

- We acquired the world's largest photoproduction dataset for $\phi\,\eta$
  - 909 ± 45 $\phi\,\eta$ events
- First cross section measurement for '$\gamma\, p \rightarrow p\, X \rightarrow p\, \phi\, \eta$'
  - 5.8 ± 0.3 (stat) $\pm$ 0.72 (sys) nb for $E_\gamma \in \{4.40, 5.45\}$
- No statistically significant resonant structure observed in $\phi\,\eta$ invariant mass distribution
- First calculations of upper limits on '$\gamma\, p \rightarrow p\, X \rightarrow p\, \phi\, \eta$'
  - Upper limit for $\phi(1680)$ - 140 pb
  - Upper limit for $\phi_3(1850)$ - 60 pb
  - Upper limit for X(1750) supports X(1750) $\notin \{s\bar{s}\} \not\equiv \phi(1680)$
  - Largest cross section upper limit is observed to be 250 pb
- Strangeonia photoproduction cross sections - measured in their golden decay mode $\phi\,\eta$ - are much lower than expected
  - Assumptions of this analysis are suspect
  - Strangeonia are rarer than expected; more statistics needed
  - Search for strangeonia continues...

- We acquired the world's largest photoproduction dataset for $\phi\,\eta$
  - 909 $\pm$ 45 $\phi\,\eta$ events
- First cross section measurement for '$\gamma\, p \rightarrow p\, X \rightarrow p\, \phi\, \eta$'
  - 5.8 $\pm$ 0.3 (stat) $\pm$ 0.72 (sys) nb for $E_\gamma \in \{4.40, 5.45\}$
- No statistically significant resonant structure observed in $\phi\,\eta$ invariant mass distribution
- First calculations of upper limits on '$\gamma\, p \rightarrow p\, X \rightarrow p\, \phi\, \eta$'
  - Upper limit for ϕ(1680) - 140 pb
  - Upper limit for ϕ_3(1850) - 60 pb
  - Upper limit for X(1750) supports X(1750) $\notin \{s\bar{s}\} \not\equiv \phi$(1680)
  - Largest cross section upper limit is observed to be 250 pb
- Strangeonia photoproduction cross sections - measured in their golden decay mode $\phi\,\eta$ - are much lower than expected
  - Assumptions of this analysis are suspect
  - Strangeonia are rarer than expected; more statistics needed
  - Search for strangeonia continues. . .

Summary

- We acquired the world's largest photoproduction dataset for $\phi\,\eta$
  - 909 ± 45 $\phi\,\eta$ events
- First cross section measurement for '$\gamma\, p \;\rightarrow\; p\, X \;\rightarrow\; p\, \phi\, \eta$'
  - 5.8 ± 0.3 (stat) $\pm$ 0.72 (sys) nb for $E_\gamma \in \{4.40, 5.45\}$
- No statistically significant resonant structure observed in $\phi\,\eta$ invariant mass distribution
- First calculations of upper limits on '$\gamma\, p \;\rightarrow\; p\, X \;\rightarrow\; p\, \phi\, \eta$'
  - Upper limit for ϕ(1680) - 140 pb
  - Upper limit for ϕ_3(1850) - 60 pb
  - Upper limit for X(1750) supports X(1750) $\notin \{s\bar{s}\} \not\equiv \phi$(1680)
  - Largest cross section upper limit is observed to be 250 pb
- Strangeonia photoproduction cross sections - measured in their golden decay mode $\phi\,\eta$ - are much lower than expected
  - Assumptions of this analysis are suspect
  - Strangeonia are rarer than expected; more statistics needed
  - Search for strangeonia continues. . .

- We acquired the world's largest photoproduction dataset for $\phi\ \eta$
  - 909 $\pm$ 45 $\phi\ \eta$ events
- First cross section measurement for '$\gamma\ p\ \rightarrow\ p\ X\ \rightarrow\ p\ \phi\ \eta$'
  - 5.8 $\pm$ 0.3 (stat) $\pm$ 0.72 (sys) nb for $E_\gamma \in \{4.40, 5.45\}$
- No statistically significant resonant structure observed in $\phi\ \eta$ invariant mass distribution
- First calculations of upper limits on '$\gamma\ p\ \rightarrow\ p\ X\ \rightarrow\ p\ \phi\ \eta$'
  - Upper limit for ϕ(1680) - 140 pb
  - Upper limit for ϕ_3(1850) - 60 pb
  - Upper limit for X(1750) supports X(1750) $\notin \{s\bar{s}\} \not\equiv \phi$(1680)
  - Largest cross section upper limit is observed to be 250 pb
- Strangeonia photoproduction cross sections - measured in their golden decay mode $\phi\ \eta$ - are much lower than expected
  - Assumptions of this analysis are suspect
  - Strangeonia are rarer than expected; more statistics needed
  - Search for strangeonia continues. . .

Summary

- We acquired the world's largest photoproduction dataset for $\phi\,\eta$
  - 909 ± 45 $\phi\,\eta$ events
- First cross section measurement for '$\gamma\, p \rightarrow p\, X \rightarrow p\, \phi\, \eta$'
  - 5.8 ± 0.3 (stat) $\pm$ 0.72 (sys) nb for $E_\gamma \in \{4.40, 5.45\}$
- No statistically significant resonant structure observed in $\phi\,\eta$ invariant mass distribution
- First calculations of upper limits on '$\gamma\, p \rightarrow p\, X \rightarrow p\, \phi\, \eta$'
  - Upper limit for $\phi(1680)$ - 140 pb
  - Upper limit for $\phi_3(1850)$ - 60 pb
  - Upper limit for X(1750) supports X(1750) $\notin \{s\bar{s}\} \not\equiv \phi(1680)$
  - Largest cross section upper limit is observed to be 250 pb
- Strangeonia photoproduction cross sections - measured in their golden decay mode $\phi\,\eta$ - are much lower than expected
  - Assumptions of this analysis are suspect
  - Strangeonia are rarer than expected; more statistics needed
  - Search for strangeonia continues. . .

To FSU Physics And Everyone Who Came

Thank You!

$$|\bar{p}\epsilon PJM\rangle = \theta(m)\ \{\ |\bar{p}PJM\rangle + \epsilon P(-1)^{J\text{-}M}\ |\bar{p}PJ - M\rangle\ \}$$

where,

$$\theta(m) = \frac{1}{\sqrt{2}}\ for\ m > 0\ ;\ \ \theta(m) = \frac{1}{2}\ for\ m = 0;$$
$$\theta(m) = 0\ \ for\ m < 0.$$

Reflectivity (ϵ) / Naturality (N) for a particle, in this case, by definition is:

$$\epsilon = N = P(-1^{J})$$

hence the following holds true,

$$\text{Natural parity exchange } \epsilon = 1; \quad J^P = 0^+, 1^-, 2^+, \ldots$$
$$\text{Unnatural parity exchange } \epsilon = \text{-}1; \quad J^P = 0^-, 1^+, 2^-, \ldots$$

As an added advantage, states of different reflectivities / naturalities do not interfere.

$$^{\epsilon}U_k(\Omega) = \sum_{lm} \epsilon V_{lmk} \sqrt{\frac{2l+1}{4\pi}}\, {^{\epsilon}D^{l}_{m0}}^{*}(\phi, \theta, 0)$$

$$I(\Omega) = \sum_{\epsilon k} \left|^{\epsilon}U_k(\Omega)\right|^2 = \left|^{+}U_1(\Omega)\right|^2 + \left|^{-}U_1(\Omega)\right|^2 + \left|^{+}U_2(\Omega)\right|^2 + \left|^{-}U_2(\Omega)\right|^2$$

$$\mathcal{M} = \sum_{\alpha,\phi} \underbrace{\langle K^+K^- \ \eta\ p|\ \hat{T}_d^{\phi\to K^+K^-}\ |\phi\ \eta\ p\rangle\ \langle \phi\ \eta\ p|\ \hat{T}_d^{X\to\phi\eta}\ |X_\alpha\ p\rangle}_{Decay-A_\alpha(\tau)} \underbrace{\langle X_\alpha\ p|\ \hat{T}_p\ |\gamma p\rangle}_{Production-V_\alpha}$$

$$I(\tau) \propto \sum_k \left|\sum_\alpha V_{k\alpha} A_\alpha(\tau)\right|^2$$

$$\alpha\ \forall\ \{J, P, C, M, L, l, (w, \Gamma)\}$$

where,

J	=	Total angular momentum of resonance 'X'
P	=	Parity of the resonance 'X'
C	=	Charge conjugation parity for the resonance 'X'
M	=	Z-projection of the total angular momentum
L	=	Angular momentum between the ϕ and the η meson
l	=	Angular momentum between the decay products of ϕ
(w, Γ)	=	Mass and width parameter for the Breit-Wigner

Extended Maximum Likelihood Method

$$\mathcal{L} \propto \left[\frac{\bar{n}^n}{n!} e^{-n}\right] \prod_i^n \left[\frac{I(\tau_i)}{\int I(\tau)\eta(\tau)pqd\tau}\right]$$

$$\bar{n} \propto \int I(\tau)\eta(\tau)pq(d\tau)$$

$$\begin{aligned} ln\mathcal{L} &\propto \sum_i^n ln(I(\tau_i)) - \int I(\tau)\eta(\tau)pqd\tau \\ &\propto \sum_{k\epsilon\alpha\alpha'} ln({}^{\epsilon}V_{\alpha k}\, {}^{\epsilon}V^*_{\alpha' k}\, {}^{\epsilon}A_{\alpha}(\tau_i)\, {}^{\epsilon}A^*_{\alpha'}(\tau_i)) - \eta_X(\sum_{k\epsilon\alpha\alpha'} {}^{\epsilon}V_{\alpha k}\, {}^{\epsilon}V^*_{\alpha' k}\, {}^{\epsilon}\psi^a_{\alpha\alpha'}) \end{aligned}$$

$$\eta_X = \frac{\text{MC Events Accepted}}{\text{Raw MC Events Generated}}$$

$${}^{\epsilon}\psi^a_{\alpha\alpha'} = \frac{1}{N_a}\sum_i^{N_a} {}^{\epsilon}A_{\alpha}(\tau_i)\, {}^{\epsilon}A^*_{\alpha'}(\tau_i)$$

$$N = \sum_{k\epsilon\alpha\alpha'} {}^{\epsilon}V_{\alpha k}\, {}^{\epsilon}V^*_{\alpha' k}\, {}^{\epsilon}\psi^r_{\alpha\alpha'}$$

where,

$\mathcal{L}$	*is*	the likelihood function,
n	*is*	the number of events observed,
$\bar{n}$	*is*	the average number of events observed if the experiment was ran multiple times,
$\eta(\tau)$	*is*	the finite experimental acceptance as determined by the Monte Carlo simulations,
$pqd\tau$	*is*	the lorentz invariant phase space element for the involved kinematics,
${}^{\epsilon}\psi^a_{\alpha\alpha'}$	*is*	the normalization integral calculated from phase space MC simulation for N_a accepted events.

$$\gamma \ + \ proton \ \rightarrowtail \ proton \ + \ \phi \ + \ \pi^0$$

$$\gamma \ + \ proton \ \rightarrowtail \ proton \ + \ K^+ \ + \ K^- \ + \ [\pi^0]$$

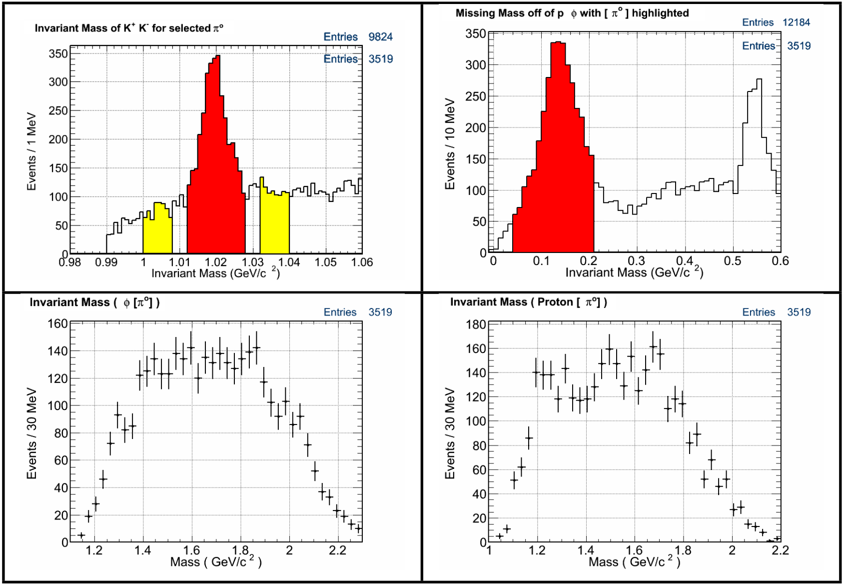

Invariant Mass of K⁺ K⁻ for selected π°
Entries 9824
Entries 3519
Events / 1 MeV
Invariant Mass (GeV/c²)
Missing Mass off of p ϕ with [π°] highlighted
Entries 12184
Entries 3519
Events / 10 MeV
Invariant Mass (GeV/c²)
Invariant Mass (ϕ [π°])
Entries 3519
Events / 30 MeV
Mass (GeV/c²)
Invariant Mass (Proton [π°])
Entries 3519
Events / 30 MeV
Mass (GeV/c²)

Sidebands

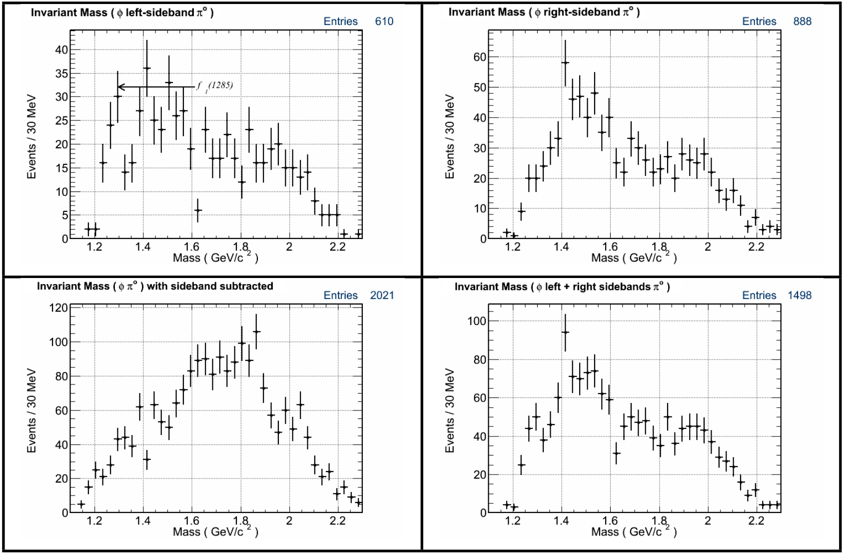

Invariant Mass (ϕ left-sideband π°)
Entries 610
f 1(1285)
Events / 30 MeV
Mass (GeV/c 2)
Invariant Mass (ϕ right-sideband π°)
Entries 888
Events / 30 MeV
Mass (GeV/c 2)
Invariant Mass (ϕ π°) with sideband subtracted
Entries 2021
Events / 30 MeV
Mass (GeV/c 2)
Invariant Mass (ϕ left + right sidebands π°)
Entries 1498
Events / 30 MeV
Mass (GeV/c 2)

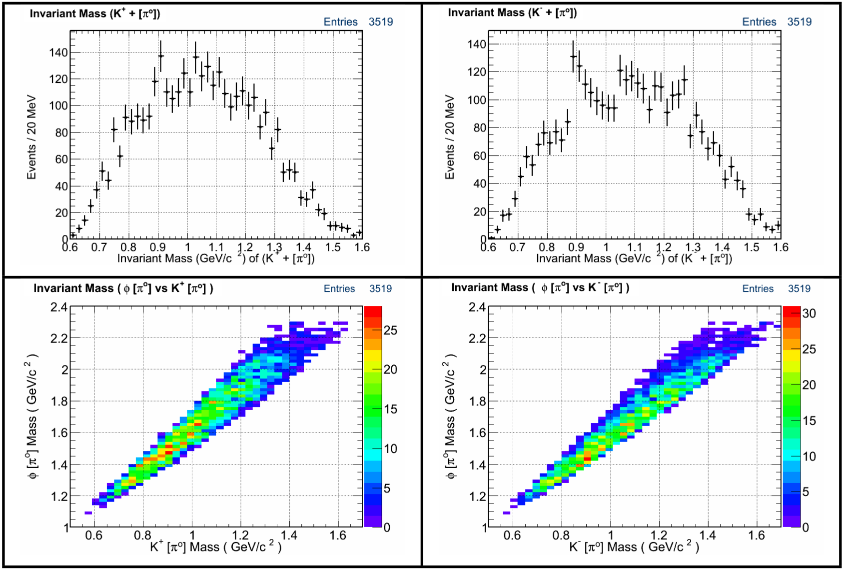

Invariant Mass (K+ + [π°])
Entries 3519
Events / 20 MeV
Invariant Mass (GeV/c 2) of (K+ + [π°])
Invariant Mass (K- + [π°])
Entries 3519
Events / 20 MeV
Invariant Mass (GeV/c 2) of (K- + [π°])
Invariant Mass (φ [π°] vs K+ [π°])
Entries 3519
φ [π°] Mass (GeV/c 2)
K+ [π°] Mass (GeV/c 2)
Invariant Mass (φ [π°] vs K- [π°])
Entries 3519
φ [π°] Mass (GeV/c 2)
K- [π°] Mass (GeV/c 2)

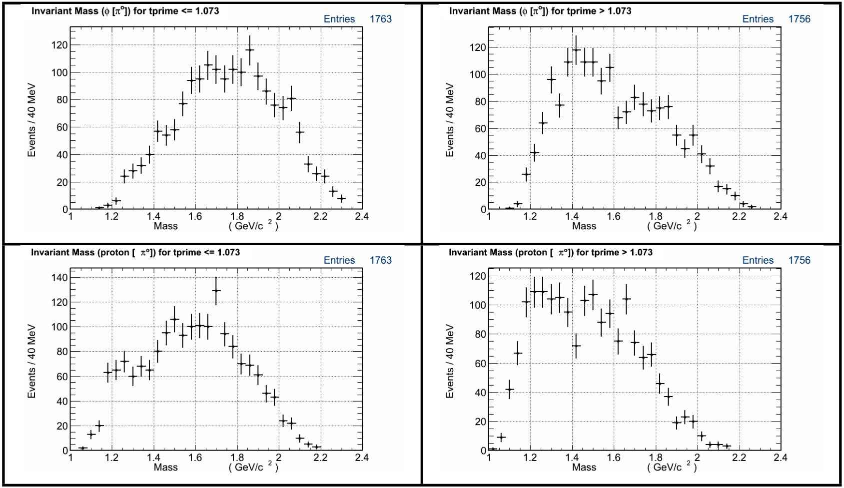
Invariant Mass (ϕ [π°]) for tprime <= 1.073
Entries 1763
Invariant Mass (ϕ [π°]) for tprime > 1.073
Entries 1756
Invariant Mass (proton [π°]) for tprime <= 1.073
Entries 1763
Invariant Mass (proton [π°]) for tprime > 1.073
Entries 1756
Events / 40 MeV
Mass
(GeV/c 2)

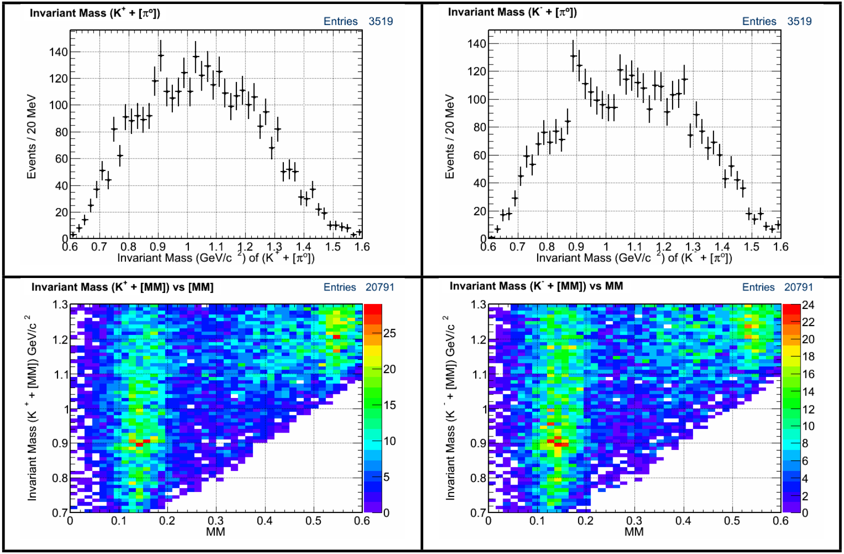
Invariant Mass (K+ + [π0])
Entries 3519
Events / 20 MeV
Invariant Mass (GeV/c 2) of (K+ + [π0])
Invariant Mass (K- + [π0])
Entries 3519
Events / 20 MeV
Invariant Mass (GeV/c 2) of (K- + [π0])
Invariant Mass (K+ + [MM]) vs [MM]
Entries 20791
Invariant Mass (K + + [MM]) GeV/c 2
MM
Invariant Mass (K- + [MM]) vs MM
Entries 20791
Invariant Mass (K - + [MM]) GeV/c 2
MM